Lyapunov-based versus Poincaré Map Analysis of the Rimless Wheel

Cenk Oguz Saglam, Andrew R. Teel and Katie Byl

***Abstract*— Hybrids systems are combinations of continuous and discrete systems. The bouncing ball is an extensively studied hybrid system, for which many solid Lyapunov-based tools are now available. Toward applying these tools to walking robots, where a hybrid dynamical system framework is also a natural fit, the rimless wheel provides a salient dynamic model because it shares commonalities with both bouncing balls and two-legged robots. While much of existing locomotion research is based on Poincaré analysis, in this paper we also study the rimless wheel using Lyapunov-based tools. Our results motivate future use of Poincaré maps for certain hybrid systems and Lyapunov-based tools for more complicated walkers.**

I. INTRODUCTION

Many dynamic systems cannot be modeled by continuous or discontinuous models alone. Hybrid dynamical systems may exhibit both continuous and discrete dynamics [1], [2], [3]. There are numerous examples, but arguably the most well-known one is a bouncing ball [4], [5]. Many aspects of this example have been studied extensively and are readily applicable to more complicated systems [6]. Of particular interest to the authors, hybrid systems research is very promising in the field of walking robots [7], for which swinging of a leg has continuous dynamics, whereas impacts are well-modeled as discrete events.

In this paper we study the rimless wheel, shown in Figure 1. After Tad McGeer's introduction of passive dynamic walking in [8] over two decades ago, the rimless wheel has become very popular in locomotion research due its simplicity while keeping many of the essential properties of walking robots. Most analyses have focused on limit cycles to determine if a given walking motion is locally stable [9]. Furthermore, results on the rimless wheel can be used to stabilize more complicated walkers [10], [11], [12]. These works show the similarities between the rimless wheel and simple walkers consisting of two legs. The rimless wheel abstraction can also be extended to include actuated spokes [13], [14] and/or 3D dynamics [15], [16].

Although the rimless wheel's connection to underactuated walking models has been noted by many locomotion researchers, its similarities with the classic bouncing ball model are not yet widely acknowledged in the literature, to our knowledge. This is important because the bouncing ball is well-studied by control theory researchers, as mentioned. As we demonstrate in this paper, the rimless wheel is a bridge between the bouncing ball and dynamic walkers. To illustrate, in all three examples, when the contact point of interest is above the ground we have continuous dynamics regulated by gravity. These dynamics are interrupted by impact events when that point contacts the ground. However, for the bouncing ball one usually studies the stability of stopping on a platform, while the focus for walkers is on stability of walking, i.e., not stopping. In this paper, we study the stability of both stopping and walking of the rimless wheel to make the connection.

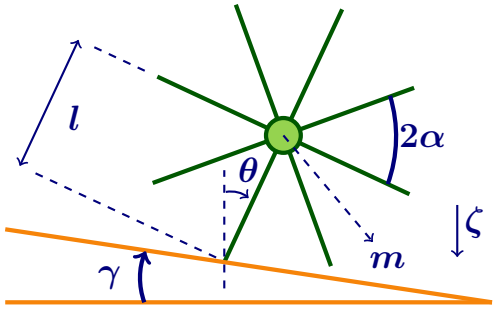

Fig. 1. The rimless wheel as depicted in [17]. We define forward direction to be to the right (i.e., clockwise) .

We look at the rimless wheel in two different ways. One approach investigates the full dynamics in terms of Lyapunov stability. This method is very general and widely used by control theory researchers. The second method involves Poincaré maps, which is a common approach used to study stability of nonlinear, limit cycle behaviors in walking robotics research [16], [18]. A Poincaré map reduces a continuous-time dynamic system by one degree and represents it as a discrete-time one, from which we can derive some information regarding the full dynamics. Arguably, the second method is easier to apply, but there is some loss of information which may or may not be important to the analysis. For both the Lyapunov and Poincaré analyses that we carry out, we study dynamic behavior on both flat (or constant-incline) terrains and changing (stochastic) slopes.

This paper aims to motivate control theory researchers to study the problem of controlling walking robots and locomotion researchers to employ existing tools within the hybrid systems field. It is a step towards closing the gap by showing that Lyapunov stability is also applicable to locomotion research and introducing a motivating example to hybrid systems researchers.

This work was supported by the Institute for Collaborative Biotechnologies through grant W911NF-09-0001 from the U.S. Army Research Office. The content of the information does not necessarily reflect the position or the policy of the Government, and no official endorsement should be inferred.

Research supported in part by AFOSR grant number FA9550-12-1-0127 and NSF grant number ECCS-1232035.

C.O. Saglam, A.R. Teel and K. Byl are with the Electrical and Computer Engineering Department, University of California, Santa Barbara, CA 93106 USA saglam@ece.ucsb.edu, teel@ece.ucsb.edu, katiebyl@ece.ucsb.edu

II. MODEL

Figure 1 illustrates the rimless wheel on an inclined terrain. When the slope is zero, i.e., $\gamma = 0$, the terrain is said to be flat. We assume the mass m is lumped into the center of the robot. The length of each leg is given by l, whereas each inter-leg angle is $2\alpha = 2\pi/N$, with N being the number of legs. For simplicity we will assume $l = 1m$ and $m = 1kg$. The gravitational acceleration ζ will be taken to be $9.81m/s^2$. We will work with $N \geq 5$, since $N \leq 4$ results in the velocity vector of the mass at impact being directed between the two contact points on the ground, which is not so useful for a rolling analysis.

The $N = 8$ case is shown in Figure 1, which also depicts angle θ. In this paper we will have $|\gamma| < \pi/2$ and we assume that legs never slip, i.e., the friction is always enough.

The single support phase is when only one leg is in contact with the ground. This phase has continuous pendulum dynamics: $\ddot{\theta} = \zeta sin(\theta)$. The leg in contact with the ground is referred to as the stance leg. On the other hand, double support phase is when two legs are in contact with the ground. This is well described as an instantaneous impact event. The jump map is obtained using conservation of momentum: $w^+ = cos(2\alpha)w$, where $w = \dot{\theta}$ is the angular velocity [8]. Thus, the rimless wheel is a hybrid dynamic system. Walking is single and double support phases following one another. A step occurs between two consecutive impacts and includes one of these impacts. (In this paper, we will arbitrarily define it to include the first of the two impacts.) Stopping will refer to velocity becoming and staying zero. Failing will mean not being able to take another step.

III. LYAPUNOV STABILITY ANALYSIS

A. Flat terrain

We will first consider flat terrain, i.e. when $\gamma = 0$. The state of the robot consists of the angle θ and angular velocity $\omega = \dot{\theta}$, i.e.,

$$x = \begin{bmatrix} x_1 \\ x_2 \end{bmatrix} = \begin{bmatrix} \theta \\ w \end{bmatrix} \in \mathbb{R}^2. \tag{1}$$

Having none of the legs below the ground level corresponds to the set

$$C_0 = \{x \in \mathbb{R}^2 : \ -\alpha \leq x_1 \leq \alpha\}. \tag{2}$$

during which the robot will follow the pendulum dynamics:

$$\dot{x} = f(x) = \begin{bmatrix} x_2 \\ \zeta sin(x_1) \end{bmatrix}. \tag{3}$$

A jump happens when two legs are in contact with the ground, and the dot product of the velocity of the mass with the normal vector pointing into the terrain is positive. The state is then in the jump set given by

$$D = \{x \in \mathbb{R}^2 : \ x_1 = -\alpha, \ x_2 \leq 0 \text{ or } x_1 = \alpha, \ x_2 \geq 0\}. \tag{4}$$

For flat terrain, the jump map is given by

$$x^+ = g(x) = \begin{bmatrix} -x_1 \\ cos(2\alpha)x_2 \end{bmatrix}. \tag{5}$$

The instantaneous change of θ is due to relabeling of the stance leg.

Next, note that $(0, 0)$ is an unstable equilibrium point for the flow map. Also, there exist initial conditions outside the origin that will arrive exactly at the origin (in infinite time). However, this is not particularly interesting nor useful for our study in this paper. So, we define the flow set as

$$C = \{x \in \mathbb{R}^2 : \ -\alpha \leq x_1 \leq \alpha, \ \sqrt{x_1^2 + x_2^2} \geq r\}, \tag{6}$$

where $r > 0$ is small. Note that the new flow set is obtained from the set in (2) by removing an open ball with radius r centered at the origin.

For this system, we will study the stability of the set

$$\mathcal{A} = \{-\alpha, \alpha\} \times \{0\}. \tag{7}$$

Physically, this set corresponds to two feet touching the ground and having zero velocity (stopping). Consider the Lyapunov function candidate

$$V(x) = \frac{1}{2}x_2^2 + \zeta(cos(x_1) - cos(\alpha)), \tag{8}$$

which represents the total energy. For $x \in C \cup D$, $V(x) = 0$ requires $x \in \mathcal{A}$ and $V(x) > 0$ for $x \notin \mathcal{A}$ because $-\alpha \leq x_1 \leq \alpha$. $V(x)$ also goes unbounded as x_2 goes unbounded. During the flows V is constant

$$\langle \nabla V(x), f(x) \rangle = x_2 \dot{x}_2 - \zeta sin(x_1)\dot{x}_1 = 0, \tag{9}$$

which is expected since it represent the total energy. Also, jumps do not cause an increase, because

$$V(g(x)) - V(x) = -\frac{1}{2}(1 - cos^2(2\alpha))x_2^2 \leq 0. \tag{10}$$

The case in which V stays constant (does not decrease) occurs only when $x_2 = 0$. But $x_2 = 0$ at jumps ($x \in D$) means $x \in \mathcal{A}$. To prove uniform global asymptotic stability of $\mathcal{A}$ (See Appendix for definition), we will use Matrosov functions for hybrid systems defined in the Appendix and explained in [19]. Starting with $V(x)$ we have a decrease in jumps for $x \notin \mathcal{A}$ and non-increasing flows. We then define $V_2(x) := -x_1 x_2$ to get

$$\langle \nabla V_2(x), f(x) \rangle = -\zeta x_1 sin(x_1) - x_2^2 < 0 \text{ for } x \in C \tag{11}$$

Then $\mathcal{A}$ is uniformly globally asymptotically stable (UGAS).

B. Inclined Terrain

Next, we look at the more general case where $-\alpha < \gamma < \alpha$. Remember that $\alpha \leq \pi/5$ since we assume $N \geq 5$ in this paper. We first define $\beta_1 := \gamma - \alpha$ and $\beta_2 := \gamma + \alpha$. Then, the flow set is given by

$$C = \{x \in \mathbb{R}^2 : \ \beta_1 \leq x_1 \leq \beta_2, \ \sqrt{x_1^2 + x_2^2} \geq r\}, \tag{12}$$

where r is small, and the jump set is

$$D = \{x \in \mathbb{R}^2 : \ x_1 = \beta_1, \ x_2 \leq 0 \text{ or } x_1 = \beta_2, \ x_2 \geq 0\}. \tag{13}$$

During flows, the system will continue acting as a pendulum as given in (3). However, the jump map given needs to be modified as

$$x^+ = g(x) = \begin{bmatrix} -x_1 + 2\gamma \\ cos(2\alpha)x_2 \end{bmatrix} \tag{14}$$

Figure 2 illustrates the state space of the robot and some typical trajectories. Note the trajectory heading to the origin stops flowing.

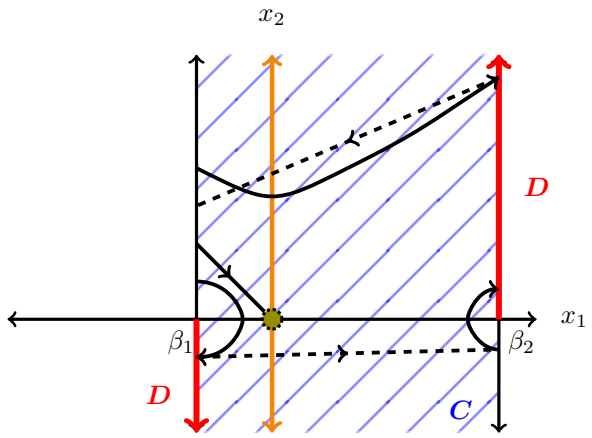

Fig. 2. State space and Poincaré section for rimless wheel when $\gamma > 0$. The vertical line at $x_1 = 0$ is when the rimless wheel is upright ($\theta = 0$ in Figure 1). Open ball at the origin with radius r is not part of the flow set. Also, in reality (β_1, x_2) and (β_2, x_2) correspond to the same point. For the trajectories, solid lines represent flows, whereas the dashed lines show jumps.

We will next consider the stability of

$$\mathcal{A} = \{\beta_1, \beta_2\} \times \{0\} \tag{15}$$

on inclined terrain. To bookkeep where the next impact with the ground will occur we introduce variable ρ. If the next impact will be to the right (left), ρ will be 1 (-1). Otherwise, the walker will head toward the origin and exit the set $C \cup D$ as in Figure 2. In this case it will not be relevant whether ρ is 1 or -1. We define

$$V_3(x) := \frac{1}{2}x_2^2 + \zeta(cos(x_1) - 1), \tag{16}$$

which is obtained by offsetting V to be zero at the origin. Then ρ variable can be calculated using

$$\rho = \begin{cases} \text{sgn}(x_1) & \text{if } V_3(x) < 0, \\ \text{sgn}(x_2) & \text{if } V_3(x) \geq 0. \end{cases} \tag{17}$$

So, if the robot does not have enough energy to overcome the upright position, it will have the impact on the half where it already is. Otherwise the velocity direction will determine which side the robot will hit. Just like $V(x)$, $V_3(x)$ is constant during flows. If $V_3(x) < 0$, then the robot will not be able to pass through the $x_1 = 0$ line, so $\text{sgn}(x_1)$ will not change. Otherwise (if the robot has enough energy to reach the $x_1 = 0$ line), the robot will not fall back and the velocity will always be in the same direction. As a result, ρ is constant during flows.

With ρ defined, we consider the Lyapunov function V_4 given by

$$V_4(x) = \begin{cases} \frac{1}{2}x_2^2 + \zeta(cos(x_1) - cos(\beta_1)) & \text{if } \rho = -1, \\ \frac{1}{2}x_2^2 + \zeta(cos(x_1) - cos(\beta_2)) & \text{if } \rho = 1. \end{cases} \tag{18}$$

V_4 corresponds to the total energy with respect to the next impact point. In other words, V_4 is V shifted by a constant such that it will have zero potential energy at the next impact. Since ρ will not change during flows, $V_4(x)$ is continuous and continuously differentiable during flows.

When $V_3(x) \geq 0$, we have $x_2^2/2 \geq \zeta(1 - cos(x_1))$. This implies

$$\begin{aligned} V_4(x) &\geq \zeta(1 - cos(\beta_1)) > 0 \quad \text{if } \rho = -1, \\ V_4(x) &\geq \zeta(1 - cos(\beta_2)) > 0 \quad \text{if } \rho = 1, \end{aligned} \tag{19}$$

because $-\alpha < \gamma < \alpha$. On the other hand, if $V_3(x) < 0$, then $x_1 \neq 0$, because $x^2/2 \geq 0$. In this case (18) implies

$$\begin{aligned} V_4(x) &\geq \frac{1}{2}x_2^2 + \zeta(cos(x_1) - cos(\beta_1)) \quad \text{if } x_1 < 0, \\ V_4(x) &\geq \frac{1}{2}x_2^2 + \zeta(cos(x_1) - cos(\beta_2)) \quad \text{if } x_1 > 0, \end{aligned} \tag{20}$$

where right hand-sides are positive for $x \notin \mathcal{A}$, because $\beta_1 \leq x_1 \leq \beta_2$.

So $V_4(x) > 0$ for $x \notin \mathcal{A}$ and $V_4(x) = 0$ implies $x \in \mathcal{A}$. Furthermore, we have unboundedness of $V_4(x)$ as x_2 goes unbounded and the flows still do not change the value of V_4 as in (9). We then look at jumps, where we either have $x_1 = \beta_1$ or $x_1 = \beta_2$.

1) Jump at $x_1 = \beta_2$: In this case we have $\rho = 1$.

If $V_3(g(x)) < 0$, then $\rho^+ = -1$ because $x_1^+ = \beta_1$. This corresponds to the robot not being able to take another forward step and falling back. Then,

$$V_4(g(x)) - V_4(x) = -\frac{1}{2}x_2^2(1 - cos^2(2\alpha)) < 0. \tag{21}$$

On the other hand, $V_3(g(x)) \geq 0$ means

$$V_3(g(x)) = \frac{1}{2}cos^2(2\alpha)x_2^2 + \zeta(cos(\beta_1) - 1) \geq 0, \tag{22}$$

or equivalently

$$x_2 \geq \sqrt{2\zeta(1 - cos(\beta_1))/cos^2(2\alpha)} =: x_2^{thr1} > 0. \tag{23}$$

So, in this case we have $\rho^+ = 1$. Using (22) we obtain

$$\begin{aligned} &V_4(g(x)) - V_4(x) = -\frac{x_2^2}{2}(1 - cos^2(2\alpha)) + \zeta(cos(\beta_1) - cos(\beta_2)) \\ &\leq \frac{-\zeta}{cos^2(2\alpha)}(-cos^2(2\alpha)(1 - cos(\beta_2) + (1 - cos(\beta_1)) \end{aligned} \tag{24}$$

which is negative when

$$\frac{1 - cos(\beta_1)}{1 - cos(\beta_2)} > cos^2(2\alpha). \tag{25}$$

This is satisfied when the slope is smaller than some threshold value, i.e., $\gamma < \gamma_{thr}$.

2) Jump at $x_1 = \beta_1$: Using similar arguments we conclude that $V_4(g(x)) - V_4(x) < 0$ for

$$\frac{1 - cos(\beta_2)}{1 - cos(\beta_1)} > cos^2(2\alpha), \tag{26}$$

which corresponds to having $-\gamma_{thr} < \gamma$.

So if $-\gamma_{thr} < \gamma < \gamma_{thr}$, then we have decrease in jumps. Using functions $V_4(x)$ and $V_2(x) = -x_1 x_2$ we establish uniform global asymptotic stability as in (11).

On the other hand, let's consider all $0 \leq \gamma < \alpha$. For $V_3(g(x)) \geq 0$ we note from the first line of (24) that smaller x_2 means larger $V_4(g(x)) - V_4(x)$. In fact, we have $V_4(g(x)) > V_4(x)$ for

$$x_2 < \sqrt{\frac{2\zeta(cos(\beta_1) - cos(\beta_2))}{1 - cos^2(2\alpha)}} =: x_2^{thr2} \geq 0. \tag{27}$$

x_2^{thr1} and x_2^{thr2} are plotted on Figure 3, where $N = 8$ is assumed and y-axis is the x_2 at the impact. γ_{thr} ($= 3.909°$ for $N = 8$) is where the two lines meet. Below the x_2^{thr1} line, $V_3(g(x)) < 0$ and jump results with a decrease in V_4 for $x_2 \neq 0$ as in (21). However, points above the x_2^{thr1} line will tend to the x_2^{thr2} line vertically. This is because if $x_2^{thr1} < x_2 < x_2^{thr2}$, there will be an increase and if $x_2 > x_2^{thr2}$, there will be a decrease in V_4 from (24). The reason why $\mathcal{A}$ is UGAS for $0 \leq \gamma < \gamma_{thr}$ is because $x_2^{thr2} < x_2^{thr1}$ in this region. The case when $-\alpha < \gamma < 0$ is similar.

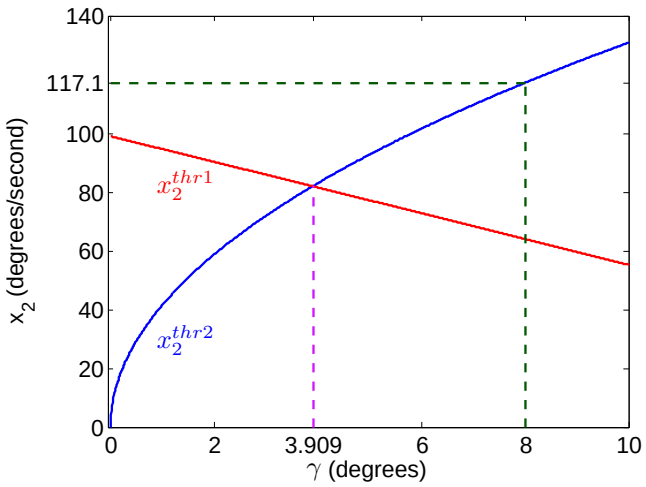

Fig. 3. x_2^{thr1} versus x_2^{thr1} for $0 \leq \gamma \leq 10°$. $x_2 = 117.1$ corresponds to the fixed point for $\gamma = 8°$ in Poincaré map as we will see later.

As a side note, when $\alpha < |\gamma| < \pi/2$, the robot will keep walking forever, no matter what the initial condition is. This corresponds to cases in which the center of mass will always lie outside the support polygon.

Finally, some approximate γ_{thr} values depending on N are given in Table I. When $N = 4$, we have $cos(2\alpha) = 0$. So a jump will cause velocity to become zero and any slope satisfying $-\alpha < \gamma < \alpha$ would preserve stability. Note that as $N \to \infty$, $\cos(2\alpha) \to 1$ (impacts cause no energy loss) and we have a wheel, rolling forever

TABLE I

APPROXIMATE THRESHOLD SLOPES IN DEGREES

N	4	5	6	7	8	1e3
$\approx \gamma_{thr}$	45	19.464	10.207	6.060	3.909	1.776×10^{-6}

C. Changing Slopes

Next, we allow the slope to change at every jump. While flowing, the system will have a particular slope in front, which we will refer to with our original symbol, γ. In addition, the slope on the back (to the left) will be denoted by γ_b. In this case, we redefine $\beta_1 := \gamma_b - \alpha$ and the state becomes four dimensional, i.e.,

$$x = \begin{bmatrix} x_1 \\ x_2 \\ x_3 \\ x_4 \end{bmatrix} = \begin{bmatrix} \theta \\ w \\ \gamma \\ \gamma_b \end{bmatrix} \in \mathbb{R}^4. \tag{28}$$

After redefining β_1, the flow and jump sets will remain as given in (12) and (13), except we will have $x \in \mathbb{R}^4$. The flow and jump maps will remain the same for x_1 and x_2. In addition we have $\dot{\gamma} = 0$, $\dot{\gamma}_b = 0$ and

$$\begin{bmatrix} \gamma^+ \\ \gamma_b^+ \end{bmatrix} = \begin{cases} \begin{bmatrix} \gamma_b \\ \gamma_{new} \end{bmatrix} & \text{if } x_1 = \beta_1, \\ \begin{bmatrix} \gamma_{new} \\ \gamma \end{bmatrix} & \text{if } x_1 = \beta_2, \end{cases} \tag{29}$$

where γ_{new} is a random variable, drawn at each impact.

We adopt the Lyapunov function in (18) and look at the stability of $\mathcal{A} = \{\beta_1, \beta_2\} \times \{0\}$. Assume $\gamma_{new} \in (-\gamma_{thr}, \gamma_{thr})$, where γ_{thr} is as calculated in the previous section. As a result,

$$\frac{1 - cos(\beta_2)}{1 - cos(\beta_1)} > \frac{1 - cos(-\gamma_{thr} + \alpha)}{1 - cos(-\gamma_{thr} - \alpha)} = cos^2(2\alpha) \tag{30}$$

$$\frac{1 - cos(\beta_1)}{1 - cos(\beta_2)} > \frac{1 - cos(\gamma_{thr} - \alpha)}{1 - cos(\gamma_{thr} + \alpha)} = cos^2(2\alpha) \tag{31}$$

So we still have decrease at jumps when $x \notin \mathcal{A}$, as in (24). Using the same Matrosov functions of the previous section we conclude that $\mathcal{A} = \{\beta_1, \beta_2\} \times \{0\}$ is still UGAS, given $\gamma_{new} \in (-\gamma_{thr}, \gamma_{thr})$. If $\gamma_{new} \in (\gamma_{thr}, \pi/2)$, then with appropriately enough forward energy, the robot will always walk. What is even more interesting is what happens when such guarantees on γ_{new} cannot be made. We address this issue next.

D. Stochastic Terrain

In this section, we look at the stochastic terrain problem and apply tools presented in [20]. As $N \leq 4$ is a trivial case, we will look at $N \geq 5$, but finite. We will assume γ_{new} is generated by an independent and identically distributed (i.i.d.) sequence of random variables, which also generate a

probability distribution μ. We will assume the support of this distribution is the set of angles between $-\pi/2$ and $\pi/2$, i.e.,

$$\mu((-\pi/2, \pi/2)) = 1. \tag{32}$$

We further assume that

$$cos^2(2\alpha) < \int_{\mathbb{R}} \frac{1 - cos(\gamma_{new} + \alpha)}{1 - cos(\gamma_{new} - \alpha)} \mu(d\gamma_{new}) < 1/cos^2(2\alpha). \tag{33}$$

We then consider the Lyapunov function $V_4(x)$ defined in (18). As before, we have non-increasing flows. Moreover, if $x_1 = \beta_1$ or $x_1 = \beta_2$, we may have an increase or decrease at a single jump with constraint (33). However, we wish to consider the behavior when γ_{new} is generated by an independent and identically distributed (i.i.d.) sequence of random variables. In this case, if $x_1 = \beta_2$ and $\rho^+ = 1$, then

$$\begin{aligned} &\int_{\mathbb{R}} (V_4(g(x)) - V_4(x)) \mu(d\gamma_{new}) \\ &\leq \frac{-\zeta}{cos^2(2\alpha)} \int_{\mathbb{R}} \frac{1}{(1 - cos(\gamma_{new} + \alpha))} \\ &\left(\frac{1 - cos(\gamma_{new} - \alpha)}{1 - cos(\gamma_{new} + \alpha)} - cos^2(2\alpha) \right) \mu(d\gamma_{new}), \end{aligned} \tag{34}$$

which is negative for the assumption in (33). We similarly obtain negativeness for $x_1 = \beta_1$ case too. We repeat the Matrosov analysis carried in the previous parts and then refer to [20] to conclude set $\mathcal{A}$ is UGAS in probability.

IV. POINCARÉ MAP STABILITY

In the previous section, we studied Lyapunov stability of the full hybrid dynamics of the rimless wheel. Remember that the state space of the robot is shown in Figure 2. Now, we will first select a Poincaré section. Although there are numerous other possibilities, we found choosing the (vertical) line $x_1 = 0$ to be most helpful. We will restrict our attention to forward motion, which will make analysis easier while not losing any point we want to show. We will be working on the system described for changing slopes. The emphasis in this section will be on the stability of walking. We will also assume $-\pi/2 < \gamma < \pi/2$ and the robot starts in $x_1 = 0$ position with $x_2 > 0$. This initial velocity is denoted by w_0. More generally, w_n denotes the velocity after n steps are taken. Given, $w_n > 0$ and $w_{n+1} \geq 0$, we have the following relationship

$$w_{n+1} = \sqrt{cos^2(2\alpha)(w_n^2 + 2\zeta(1 - cos\beta_2)) - 2\zeta(1 - cos\beta_1)} \tag{35}$$

as shown in [17], which can be easily verified using the conservation of energy during the flows and conservation of angular momentum at the impacts. If the argument of the square root in the equation above is negative, then the robot did not actually intersect the Poincaré section again. This means it fell back, which will imply stability of stopping at the impact points as we saw. If, on the other hand, w_{n+1} turns out to be zero, that means the robot stopped at the upright position. In either of these cases, the robot will not be able to take another step (the robot simply failed), so we stop iterating (35). Moreover, substituting $w_{n+1} = w_n > 0$ gives $\gamma > \gamma_{thr}$, where γ_{thr} is as calculated before. In this case, the solution of the full dynamics converges to a limit cycle because the reduced dynamics converge to a fixed point as we show shortly.

Note that we look at forward walking only, thus the state is three dimensional (position, velocity and slope). Starting with a hybrid system and taking a Poincaré section we reduced this dimension to two. If the slope is constant, we have a 1D discrete system. If the slope is generated by some distribution, then we have a 1D Markov chain. For stable walking, the robot needs to keep passing though the Poincaré section. From the previous section we also know that not going through this line after some time means stopping.

Assuming $w_k > 0$ for $k = \{0, 1, ..., n\}$ and using (35) iteratively, we can write

$$w_n^2 = \eta^n w_0^2 + 2\zeta \sum_{k=0}^{n-1} \eta^{n-1-k} \psi_n, \tag{36}$$

where $\eta = cos^2(2\alpha)$, $\psi_k = \eta(1 - cos(\gamma_k + \alpha)) - (1 - cos(\gamma_k - \alpha))$ and γ_k is the slope before $(k+1)^{\text{th}}$ impact. The robot will keep walking as long as $w_n > 0$. It is destined to stop when $w_n \leq 0$ for some n. Having $\psi < 0$ corresponds to $\gamma < \gamma_{thr}$, which guarantees stability of stopping as we saw previously and can also verify by taking limit as $n \to \infty$ in (36). On the other hand, having $\sum_{k=0}^{\infty} \eta^{n-1-k} \psi_n < 0$ is also sufficient for stability of stopping, because $\eta^n \to 0$ as $n \to \infty$. It is also easy to see that $\psi_n > 0$ will result in stable walking with $w_0 > 0$. In particular, when slope is fixed, we have $\psi = \psi_n$ constant. Then,

$$w_n^2 = \eta^n w_0^2 + 2\zeta\psi \frac{1 - \eta^n}{1 - \eta}. \tag{37}$$

As $n \to \infty$, we have $w_n^2 = 2\zeta\psi/(1 - \eta)$, which shows there is a limit cycle. It is also important to note that initial condition vanishes as the robot takes steps. To the authors' experience, walking robots "almost forget" initial conditions within several steps, given they haven't stopped.

A. Metastability

As in the section on Lyapunov stability, we end this section looking at stochastic terrain. Remember in section III-D, we saw that (33) is a sufficient condition for $\mathcal{A}$ being UGAS. However, note that (33) not holding does not mean the origin $\mathcal{A}$ is not UGAS. In such cases, we wish to know how many steps are expected to be taken before failing (not intersecting Poincaré section with positive velocity). This term corresponds to Mean First Passage Time (MFPT) of [17] as we explain next.

The method in [17] requires finite and discrete slope and state sets. For the slope set we will use

$$\Gamma = \{\gamma \in \mathbb{R} : \ \gamma = (k-1)^\circ/10, \ k \in \mathbb{Z}, \ 1 \leq k \leq 161\}. \tag{38}$$

And the state set will be

$$W = \{w \in \mathbb{R} : \ w = (k-1)/100, \ k \in \mathbb{Z}, \ 1 \leq k \leq 251\}. \tag{39}$$

Let us adopt the following notation $\gamma_{\{k\}} := (k-1)/10$ and $w_{\{k\}} := (k-1)/100$. $w_{\{1\}}$ will represent the absorbing failure state. Both sets can be made denser for higher accuracy or coarser for faster computation. Because of low dimensionality, computation time is very small (less than a second). Also, the accuracy gained while calculating MFPT with denser sets was negligible. For the issue of dealing with higher dimensional systems see [21], [22].

After determining these sets, what is done is to calculate w_{n+1} for each $w_n \in W \setminus \{w_{\{1\}}\}$ and $\gamma \in \Gamma$. While doing so, we say $w_{n+1} = w_{\{1\}}$ if w_{n+1} does not turn out to be positive real. We define the closest point in set W to a point $\tilde{w}$ as

$$c(\tilde{w}, W) := \underset{w \in W}{\operatorname{argmin}} (w - \tilde{w})^2 \tag{40}$$

Let $h(w_n, \gamma)$ denote the right hand side of (35) when it is real, and $h(w_n, \gamma) = 0$ if not. We then get the deterministic state transition map calculated by

$$T_{d\{ij\}}(\gamma) = \begin{cases} 1, & \text{if } w_{\{j\}} = c(h(w_{\{i\}}, \gamma), W) \\ 0, & otherwise. \end{cases} \tag{41}$$

Next, we define the stochastic state transition matrix as

$$T_{s\{ij\}} := Pr(w_{n+1} = w_{\{j\}} \mid w_n = w_{\{i\}}). \tag{42}$$

Let $P_\Gamma(\gamma_{\{k\}})$ denote the probability of slope being $\gamma_{\{k\}}$. Then the stochastic state transition matrix can be calculated by

$$T_s = \sum_{\gamma_{\{k\}} \in \Gamma} P_\Gamma(\gamma_{\{k\}})\ T_d(\gamma_{\{k\}}) \tag{43}$$

Given the stochastic state transition matrix, the average steps to failure, or Mean First Passage Time (MFPT), is

$$M = \frac{1}{1 - \lambda_2} \tag{44}$$

where λ_2 is the second largest eigenvalue of T_s. For details, we refer interested reader to [23], [17].

To illustrate, we will assume normal distribution for slopes, i.e., $\gamma_{\{k\}} \sim \mathcal{N}(\mu, \sigma^2)$, where μ is the mean and σ is the standard deviation. For each μ and σ we get a MFPT as shown in Figure 4. As mean increases and standard deviation decreases the MFPT rises. This is expected since in this case small slopes occur less frequently.

V. CONCLUSION

In this paper we studied the rimless wheel. This is a hybrid dynamical system, since it has both continuous and discontinuous dynamics. We showed uniform global asymptotic stability of stopping with two legs in contact with the ground using a Lyapunov-based approach. We also showed that a Poincaré section method is an easy but useful alternative tool. We derived results verifying what is learned with the Lyapunov based approach. For both approaches, we also looked at the stochastic terrain case. Metastability analysis showed that for a robot destined to fail taking steps eventually, the mean number of steps taken is a very useful measure.

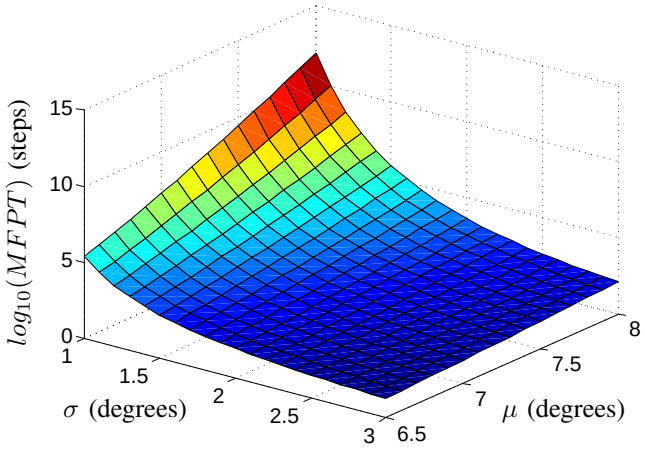

Fig. 4. Mean First Passage time as a function of slope distribution

APPENDIX - HYBRID SYSTEMS REVIEW

In this section we will provide definitions for hybrid systems explained in [6], [19] to be self-contained. We begin with some notation.

Let S be a set for the following notations. $\overline{S}$ denotes the closure of S. Given a point $x \in \mathbb{R}^n$, $|x|_S := inf_{y \in S}|x - y|$. For constants $0 \geq \delta \geq \Delta$, $\Omega_S(\delta, \Delta) := \{x \in \mathbb{R}^n : \ \delta \leq |x|_S \leq \Delta\}$. A function $\alpha : \mathbb{R}_{\geq 0} \to \mathbb{R}_{\geq 0}$ belongs to class-$\mathcal{K}_\infty$ if it is continuous, zero at zero, strictly increasing, and unbounded.

A set-valued mapping M from $S_1 \subset \mathbb{R}^m$ to $S_2 \subset \mathbb{R}^n$, denoted by $M : S_1 \rightrightarrows S_2$, associates every point $x \in S_1$ to a subset of S_2. The domain of $M : S_1 \rightrightarrows S_2$ is given by

$$\text{dom } M = \{x \in S_1 : \ M(x) \neq \emptyset\}. \tag{45}$$

We will represent hybrid systems in $\mathbb{R}^n$ in the following form

$$\begin{aligned} \dot{x} &\in F(x) \qquad x \in C \\ x^+ &\in G(x) \qquad x \in D \end{aligned} \tag{46}$$

where $x \in \mathbb{R}^n$ is the state, $C \subset \mathbb{R}^n$ is the flow set, $D \subset \mathbb{R}^n$ is the jump set, $F : \mathbb{R}^n \rightrightarrows \mathbb{R}^n$ with $C \subset$ dom F is the flow map and $G : \mathbb{R}^n \rightrightarrows \mathbb{R}^n$ with $D \subset$ dom G is the jump map. Note that $\dot{x} = f(x)$ and $x^+ = g(x)$ are special cases for this setting, where f and g are functions.

Set $E \subset \mathbb{R}_{\geq 0} \times \mathbb{N}$ is a compact hybrid domain if

$$E = \bigcup_{j=0}^{J-1} ([t_j, t_{j+1}] \times \{j\}) \tag{47}$$

for some finite sequence of times $0 = t_0 \leq t_1 \leq t_2 \leq ... \leq t_j$. E is a hybrid time domain if for each $(T, J) \in E$, $E \cap ([0, T] \times \{0, 1, ..., J\})$ is a compact hybrid time domain.

A function $\phi : E \to \mathbb{R}^n$ is a hybrid arc if E is a hybrid time domain and $t \mapsto \phi(t, j)$ is locally absolutely continuous for each $j \in \mathbb{N}$. It is complete if dom ϕ is unbounded.

A solution to the hybrid system in consideration is a hybrid arc $\phi : \text{dom } \phi \to \mathbb{R}^n$ such that

1) if $(t_1, j), (t_2, j) \in \text{dom } \phi$ with $t_2 > t_1$, then for almost all $t \in [t_1, t_2]$, $\phi(t, j) \in C$ and $\dot{\phi}(t, j) \in F(\phi(t, j))$.

2) if $(t, j), (t, j + 1) \in \text{dom } \phi$, then $\phi(t, j) \in D$ and $\phi(t, j + 1) \in G(\phi(t, j))$.

A compact set $\mathcal{A} \subset \mathbb{R}^n$ is

- uniformly globally stable (UGS) if there exists a class-$\mathcal{K}_\infty$ function α such that any solution ϕ satisfies $|\phi(t, j)|_\mathcal{A} \leq \alpha(|x(0, 0)|_\mathcal{A})$ for all $(t, j) \in \text{dom } \phi$
- uniformly globally attractive (UGA) if for each $\varepsilon > 0$ and $r > 0$ there exists $T > 0$ such that, for any solution ϕ, $|\phi(0, 0)|_\mathcal{A} \leq r$, $(t, j) \in \text{dom } \phi$ and $t + j \geq T$ imply $|\phi(t, j)|_\mathcal{A} \leq \varepsilon$
- uniformly globally asymptotically stable (UGAS) if it is both UGS and UGA.

The closed set $\mathcal{A} \subset \mathbb{R}^n$ is uniformly globally stable if there exists a function $V : \mathbb{R}^n \to \mathbb{R}_{\geq 0}$ continuously differentiable on an open set containing $\overline{C}$ and

$$\begin{aligned} V(x) = 0 \Leftrightarrow x \in \mathcal{A} \text{ and } V(x) \to \infty \text{ as } |x| \to \infty \\ \langle \nabla V(x), f(x) \rangle \leq 0 \qquad \forall x \in C,\ f \in F(x) \\ V(g) - V(x) \leq 0 \qquad \forall x \in D,\ f \in G(x) \end{aligned} \tag{48}$$

(hybrid nested Matrosov) A compact and uniformly globally stable set $\mathcal{A} \subset \mathbb{R}^n$ is uniformly globally asymptotically stable if there exists $m \in \mathbb{Z}_{\geq 1}$ and for each $0 < \delta < \Delta$

- a number $\mu > 0$
- continuous functions $u_{c,i} : \overline{C} \cap \Omega_\mathcal{A}(\delta, \Delta) \to \mathbb{R}$, $u_{d,i} : \overline{D} \cap \Omega_\mathcal{A}(\delta, \Delta) \to \mathbb{R}$, $i = \{1, ..., m\}$
- functions $V_i : \mathbb{R}^n \mathcal{A} \to \mathbb{R}$, $i = \{1, ..., m\}$, continuously differentiable on an open set containing $\overline{C} \cap \Omega_\mathcal{A}(\delta, \Delta)$, such that for each $i = \{1, ..., m\}$,

$$|V_i(x)| \leq \mu \qquad \forall x \in (\overline{C} \cup D \cup G(D)) \cap \Omega_\mathcal{A}(\delta, \Delta) \tag{49}$$

$$\langle \nabla V(x), f(x) \rangle \leq u_{c,i}(x) \qquad \forall x \in C \cap \Omega_\mathcal{A}(\delta, \Delta) \quad \forall f \in F(x) \tag{50}$$

$$V_i(g) - V_i(x) \leq u_{d,i}(x) \qquad \forall x \in D \cap \Omega_\mathcal{A}(\delta, \Delta) \quad \forall g \in G(x) \cap \Omega_\mathcal{A}(\delta, \Delta) \tag{51}$$

and, with the definitions $u_{c,0}, u_{d,0} : \mathbb{R}^n \to \{0\}$ and $u_{c,m+1}, u_{d,m+1} : \mathbb{R}^n \to \{1\}$, we have for each $j \in \{0, ..., m\}$,

1)if $x \in \overline{C} \cap \Omega_\mathcal{A}(\delta, \Delta)$ and $u_{c,i}(x) = 0$ for all $i \in \{0, ..., j\}$ then $u_{c,j+1}(x) \leq 0$,

2)if $x \in \overline{D} \cap \Omega_\mathcal{A}(\delta, \Delta)$ and $u_{d,i}(x) = 0$ for all $i \in \{0, ..., j\}$ then $u_{d,j+1}(x) \leq 0$.

REFERENCES

[1] R. Alur, C. Courcoubetis, N. Halbwachs, T. Henzinger, P.-H. Ho, X. Nicollin, A. Olivero, J. Sifakis, and S. Yovine, "The algorithmic analysis of hybrid systems," *Theoretical Computer Science*, vol. 138, no. 1, pp. 3 – 34, 1995.

[2] T. Henzinger, "The theory of hybrid automata," in *Proc. 11th Annual Symp. on Logic in Comp. Science*, Jul 1996, pp. 278–292.

[3] R. Goebel, J. P. Hespanha, A. R. Teel, C. Cai, and R. Sanfelice, "Hybrid systems: Generalized solutions and robust stability," in *Proc. of the 6th IFAC Symp. on Nonlinear Contr. Systems*, Sep. 2004.

[4] A. Lamperski and A. Ames, "Lyapunov-like conditions for the existence of zeno behavior in hybrid and lagrangian hybrid systems," in *Decision and Control, 2007 46th IEEE Conference on*, Dec 2007, pp. 115–120.

[5] Y. Or and A. Teel, "Zeno stability of the set-valued bouncing ball," *Automatic Control, IEEE Transactions on*, vol. 56, no. 2, pp. 447–452, Feb 2011.

[6] R. Goebel, R. Sanfelice, and A. Teel, *Hybrid Dynamical Systems: Modeling, Stability, and Robustness*. Princeton University Press, 2012.

[7] A. Teel, R. Goebel, B. Morris, A. Ames, and J. Grizzle, "A stabilization result with application to bipedal locomotion," in *Decision and Control (CDC), 2013 IEEE 52nd Annual Conference on*, Dec 2013, pp. 2030–2035.

[8] T. McGeer, "Passive dynamic walking," *Internation Journal of Robotics Research*, vol. 9, no. 2, pp. 62–82, 1990.

[9] I. R. Manchester, M. M. Tobenkin, M. Levashov, and R. Tedrake, "Regions of Attraction for Hybrid Limit Cycles of Walking Robots," *ArXiv e-prints*, Oct. 2010.

[10] F. Asano and Z.-W. Luo, "Asymptotically stable biped gait generation based on stability principle of rimless wheel," *Robotica*, vol. 27, no. 6, pp. 949–958, Oct. 2009. [Online]. Available: http://dx.doi.org/10.1017/S0263574709005372

[11] F. Asano, "Dynamic gait generation of telescopic-legged rimless wheel based on asymmetric impact posture," in *Humanoid Robots, 2009. Humanoids 2009. 9th IEEE-RAS International Conference on*, Dec 2009, pp. 68–73.

[12] R. M. Alexander, "Energy-saving mechanisms in walking and running," *Journal of Experimental Biology*, vol. 160, no. 1, pp. 55–69, 1991.

[13] J. Yan and S. Agrawal, "Rimless wheel with radially expanding spokes: dynamics, impact, and stable gait," in *Robotics and Automation, 2004. Proceedings. ICRA '04. 2004 IEEE International Conference on*, vol. 4, April 2004, pp. 3240–3244 Vol.4.

[14] K. Shankar and J. Burdick, "Motion planning and control for a tethered, rimless wheel differential drive vehicle," in *Intelligent Robots and Systems (IROS), 2013 IEEE/RSJ International Conference on*, Nov 2013, pp. 4829–4836.

[15] A. Smith and M. Berkemeier, "The motion of a finite-width rimless wheel in 3d," in *Robotics and Automation, 1998. Proceedings. 1998 IEEE International Conference on*, vol. 3, May 1998, pp. 2345–2350 vol.3.

[16] M. J. Coleman, A. Chatterjee, and A. Ruina, "Motions of a rimless spoked wheel: a simple 3D system with impacts," in *Dynamics and Stability of Systems*, 1997, pp. 139–160.

[17] K. Byl and R. Tedrake, "Metastable walking machines," *Int. J. of Robotics Research*, vol. 28, pp. 1040–1064, Aug 2009.

[18] R. L. Tedrake, "Applied optimal control for dynamically stable legged locomotion," Ph.D. dissertation, MIT, 2004.

[19] A. Teel, "A matrosov theorem for adversarial markov decision processes," *Automatic Control, IEEE Transactions on*, vol. 58, no. 8, pp. 2142–2148, Aug 2013.

[20] A. R. Teel, "Lyapunov conditions certifying stability and recurrence for a class of stochastic hybrid systems," *Annual Reviews in Control*, vol. 37, no. 1, pp. 1 – 24, 2013.

[21] C. O. Saglam and K. Byl, "Switching policies for metastable walking," in *Decision and Control (CDC), 2013 IEEE 52nd Annual Conference on*, Dec 2013, pp. 977–983.

[22] C. O. Saglam and K. Byl, "Robust policies via meshing for metastable rough terrain walking," in *Proceedings of Robotics: Science and Systems*, Berkeley, USA, 2014.

[23] C. O. Saglam and K. Byl, "Metastable Markov chains," in *IEEE Conference on Decision and Control (CDC)*, Dec. 2014, accepted for publication.